Title

Ashley N Campbell [*], **Charles Pepe-Ranney** [†], **and Daniel H Buckley** [†]

[*]Department of Microbioloby, Cornell University, New York, USA, and [†]Department of Crop and Soil Sciences, Cornell University, New York, USA

Abstract

We describe a novel approach for identifying microbial contributions to soil C-cycling dynamics using nucleic acid stable isotope probing coupled with next generation sequencing (SIP-NGS). In a series of parallel soil microcosms we amended soils with a complex mixture of model carbon (C) substrates and inorganic nutrients common to plant biomass, where a single C constituent is substituted for its ^{13}C-labeled equivalent. Using this approach we assessed incorporation of ^{13}C-xylose or ^{13}C-cellulose as proxies for labile soluble C and polymeric insoluble C utilization, respectively. Using CsCl gradient fractionation, incorporation of ^{13}C into DNA was measured over 30 days. The 16S rRNA gene sequences from CsCl gradient fractions were characterized by 454 pyrosequencing and classified into Operational Taxonomic Units (OTU). We describe specific patterns of C-assimilation by discrete OTUs as a function of substrate, time, and level of isotope incorporation. Incorporation of ^{13}C from xylose into OTUs was observed at days 1, 3, and 7, while notable incorporation of ^{13}C from cellulose was observed only after day 14. Of over 6,000 OTUs detected, a total of 43 and 35 unique OTUs significantly assimilated ^{13}C from xylose and cellulose, respectively. We did not observe consistent C utilization at the phylum level although both xylose and cellulose utilization were observed across 7 phyla each revealing a high diversity of bacteria able to utilize these substrates. OTUs that assimilate xylose and those that assimilate cellulose are largely mutually exclusive. Xylose assimilating OTUs are more abundant in the microbial community than cellulose assimilating OTUs, while cellulose OTUs demonstrate a greater substrate specificity than xylose OTUs. Furthermore, the increased depth provided by SIP-NGS allowed us to identify several novel cellulose utilizing bacteria.

monolayer | structure | x-ray reflectivity | molecular electronics

Abbreviations: SAM, self-assembled monolayer; OTS, octadecyltrichlorosilane

Introduction

We have only a rudimentary understanding of carbon flow through soil microbial communities. This deficiency is driven by the staggering complexity of soil microbial food webs and the opacity of these biological systems to current methods for describing microbial metabolism in the environment. Relating community composition to overall soil processes, such as nitrification and denitrification, which are mediated by defined functional groups has been a useful approach. However, carbon-cycling processes have proven more recalcitrant to study due to the wide range of organisms participating in these reactions and our inability to discern diagnostic functional genetic markers.

Excluding plant biomass, there are 2,300 Pg of carbon (C) stored in soils worldwide which accounts for ∼80% of the global terrestrial C pool BATJES, 1996; Amundson, 2001. When organic C from plants reaches soil it is degraded by fungi, archaea, and bacteria. This C is rapidly returned to the atmosphere as CO_2 or remains in the soil as humic substances that can persist up to 2000 years Yanagita, 1990. The majority of plant biomass C in soil is respired and produces 10 times more CO_2 than anthropogenic emissions on an annual basis Chapin, 2002. Global changes in atmospheric CO_2, temperature, and ecosystem nitrogen inputs, are expected to impact primary production and C inputs to soils Groenigen *et al.*, 2006 but it remains difficult to predict the response of soil processes to anthropogenic change DAVIDSON *et al.*, 2006. Current climate change models concur on atmospheric and ocean C predictions but not terrestrial Friedlingstein *et al.*, 2006. These contrasting terrestrial ecosystem model predictions reflect how little is known about soil C cycling dynamics and it has been suggested that incosistencies in terrestial modeling could be improved by elucidating the relationship between dissolved organic carbon and microbial communities in soils Neff and Asner, 2001.

An estimated 80-90% of C cycling in soil is mediated by microorganisms Nannipieri *et al.*, 2003a; n.d. Understanding microbial processing of nutrients in soils presents a special challenge due to the hetergeneous nature of soil ecosystems and methods limitations. Soils are biologically, chemically, and physically complex which affects microbial community composition, diversity, and structure Nannipieri *et al.*, 2003a. Confounding factors such as physical protection/aggregation, moisture content, pH, temperature, frequency and type of land disturbance, soil history, mineralogy, N quality and availability, and litter quality have all been shown to affect the ability of the soil microbial community to access and metabolize C substrates Sollins *et al.*, 1996; Kalbitz *et al.*, 2000. Further, rates of metabolism are often measured without knowing the identity of the microbial species involved Nannipieri *et al.*, 2003b leaving the importance of community membership towards maintaining ecosystem functions unknown Nannipieri *et al.*, 2003b; Allison and Martiny, 2008; Schimel and Schaeffer, 2012. Litter bag experiments have shown that the community composition of soils can have quantitative and qualitative impacts on the breakdown of plant materials Schimel, 1995. Reciprocal exchange of litter type and microbial inocula under controlled environmental conditions reveals that differences in community composition can account for 85% of the variation in litter carbon mineralization Strickland *et al.*, 2009. In addition, assembled communities of cellulose degraders reveal that the composition of the community has significant impacts on the rate of cellulose degradation Wohl *et al.*, 2004.

An important step in understanding soil C cycling dynamics is to identify individual contributions of discrete microorganisms and to investigate the relationship between genetic diversity, community structure, and function O'Donnell *et al.*, 2002. The vast majority of microorganisms continue to resist cultivation in the laboratory, and even when cultivation is achieved, the traits expressed by

a microorganism in culture may not be representative of those expressed when in its natural habitat. Stable-isotope probing (SIP) provides a unique opportunity to link microbial identity to activity and has been utilized to expand our knowledge of a myriad of important biogeochemical processes Chen and Murrell, 2010. The most successful applications of this technique have identified organisms which mediate processes performed by a narrow set of functional guilds such as methanogens Lu, 2005. The technique has been less applicable to the study of soil C cycling because of limitations in resolving power as a result of simultaneous labeling of many different organisms in the community. Additionally, molecular applications such as TRFLP, DGGE, and cloning that are frequently used in conjunction with SIP provide insufficient resolution of taxon identity and depth of coverage. We have developed an approach that employs a complex mixture of substrates added to soil at a low concentration relative to soil organic matter pools along with massively parallel DNA sequencing. This greatly expands the ability of nucleic acid SIP to explore complex patterns of C-cycling in microbial communities with increased resolution.

A temporal cascade occurs in natural microbial communities during the plant biomass degradation in which labile C degradation preceeds polymeric C Hu and Bruggen, 1997; Rui *et al.*, 2009. The aim of this study is to track the temporal dynamics of C assimilation through discrete individuals of the soil microbial community to provide greater insight into soil C-cycling. Our experimental approach employs the addition of a soil organic matter (SOM) simulant (a complex mixture of model carbon sources and inorganic nutrients common to plant biomass), where a single C constituent is substituted for its ^{13}C-labeled equivalent, to soil. Parallel incubations of soils amended with this complex C mixture allows us to test how different C substrates cascade through discrete taxa within the soil microbial community. In this study we use ^{13}C-xylose and ^{13}C-cellulose as a proxy for labile and polymeric C, respectively. Using a novel approach we couple nucleic acid stable isotope probing with next generation sequencing (SIP-NGS) to elucidating soil microbial community members responsible for specific C transformations. Amplicon sequencing of 16S rRNA gene fragments from many gradient fractions and multiple gradients make it possible to track C assimilation by hundreds of different taxa. Ultimately we identify discrete microorganisms responsible for the cycling of specific C substrates.

Results

To observe C use dynamics by the soil microbial community, we conducted a nucleic acid SIP experiment wherein xylose or cellulose carried the isotopic label, and, we assayed SSU rRNA gene content of CsCl gradient fractions using high-throughput DNA sequencing technology. We set up three soil microcosm series. Microcosms in each series were were amended with a C substrate mixture that included cellulose and xylose. The C substrate mixture approximated freshly degrading plant biomass. The same substrate mixture was added to microcosms in each series, however, for each series except the control, one substrate was substituted for its ^{13}C counterpart. In one series cellulose was ^{13}C-labeled in another xylose was ^{13}C-labeled and in the control series no sustrates were ^{13}C labeled. Microcosm amendments are shorthand identified in the following figures by the following code: "13CXPS" refers to the amendment with ^{13}C-xylose (that is ^{13}**C X**lose **P**lant **S**imulant), "13CCPS" refers to the ^{13}C-cellulose amendment and "12CCPS" refers to the amendment that only contained ^{12}C substrates. Xylose or cellulose were chosen to carry the isotopic label to contrast C assimilation for labile, soluble C (xylose) versus insoluble, polymeric C (cellulose). 5.3 mg of C substrate mixture per gram soil was added to each microcosm representing 18% of the total soil C. The mixture included 0.42

mg xylose-C and 0.88 mg cellulose-C g soil^{-1}. Microcosms were harvested at days 1, 3, 7, 14 and 30 during a 30 day incubation. ^{13}C-xylose assimilation peaked immediately and tapered over the 30 day incubation whereas ^{13}C-cellulose assimilation peaked at two weeks of (Figure 1).

We sequenced SSU rRNA gene smplicons from a total of 277 CsCl gradient fractions from 14 CsCl gradients and 12 bulk microcosm DNA samples. The SSU rRNA gene data set contained 1,376,008 total sequences. The average number of sequences per sample was 3,816 (sd 3,629) and 265 samples had over 1,000 sequences. We sequenced SSU rRNA gene amplicons from an average of 19.8 fractions per CsCl gradient (sd 0.57). The average density between fractions was 0.0040 g mL^{-1} The sequencing effort recoverd a total of 5,940 OTUs. 2,943 of the total 5,940 OTUs were observed in bulk samples. We observed 33 unique phylum and 340 unique genus annotations.

Ordination of CsCl gradient fraction OTU profiles can be used to observe fraction-level ^{13}C assimilation dynamics and membership differences. Each CsCl gradient fraction possesses a unique composition of SSU rRNA gene phylogenetic types. DNA buoyant density (BD) drives differences in CsCl gradient fraction SSU rRNA gene composition. For instance, lighter DNA is more abundant in fractions at lighter densities so DNA with lower G+C will be found in greater abundance at the light end of the CsCl gradient and vice versa. Duplicate gradients receiving only ^{12}C DNA with the same bulk or non-fractionated SSU rRNA gene phylogenetic composition would have the same overall profile of SSU rRNA gene phylogenetic types across the density gradient. We fed microcosms identical C substrate mixtures save for the identity of a ^{13}C labeled substrate, and by design, DNA from all microcosms harvested at a time point will be similar in bulk phylogenetic composition. Therefore, SSU rRNA gene profile differences between between gradients harvested at the same time are due to ^{13}C incorporation into bulk community DNA. ^{13}C-DNA shifts from its ^{12}C position towards the heavy end of the density gradient. This causes heavy fractions in gradients that received ^{13}C-DNA to be different in phylogenetic content than corresponding heavy fractions from gradients that received ^{12}C-DNA of the same bulk phylogenetic composition.

Ordination of CsCl gradient fraction phylogenetic profiles reveals differences and similarities between gradients. It's clear that microcosms incorporated ^{13}C from both ^{13}C-xylose and ^{13}C-cellulose as gradients from both ^{13}C-xylose and ^{13}C-cellulose microcosms differ from corresponding control gradients (Figure 1). These differences from control gradients are focused in the heavy fractions (Figure 1). Analysis of SSU rRNA gene surveys has greatly benefited from utilizing conventional methods for data exploration in ecology such as ordination (Lozupone and Knight, 2008). SSU rRNA gene phylogenetic profiles in CsCl gradient fractions have only recently been surveyed with high-throughput DNA sequencing technology and subsequently explored via ordination (Angel and Conrad, 2013; Verastegui *et al.*, 2014). Ordination of CsCl gradient fraction phylogenetic profiles has reveled the relative influence of buoyant density and soil type on gradient phylogenetic profile variance, however, ordination has not demonstrated isotope incorporation. Demonstrating isotope incorporation requires careful comparisons between control and labeled gradients over the same buoyant density range. By sequencing CsCl gradient fractions from both control and labeled gradients across the full density gradient with DNA harvested from microcosms at multiple time points, we can observe where in the density gradient ^{13}C isotope incorporation signal is strongest and when ^{13}C isotope incorporation begins (Figure 1). ^{13}C incorporation from xylose and cellulose is most apparent at days 1/3/7 and days 14/30, respectively (Figure 1). Moreover, labeled gradient fraction phylogenetic profiles diverge from controls most dramatically at relatively heavy buoy-

ant densities (Figure 1). Also, ^{13}C-DNA from ^{13}C-xylose microcosms is different in phylogenetic composition from ^{13}C-cellulose microcosm ^{13}C-DNA indicating that xylose and cellulose were assimilated by different microbial community members (Figure 1). Lastly, ordination indicates ^{13}C-xylose responders change in phylogenetic type over incubation days 1, 3 and 7 (Figure 1).

^{13}**C from cellulose was assimilated by canonical cellulose-degrading and uncharacterized microbial lineages in many phyla including Chloroflexi and Verrucomicrobia.** Isotope incorporation by an OTU is revealed by enrichment of the OTU in heavy CsCl gradient fractions containing ^{13}C labeled DNA relative to heavy fractions from control gradients containing no ^{13}C labeled DNA. We refer to OTUs that putatively incorporated ^{13}C into DNA from an isotopically labeled substrate as a substrate "responder". Only 2 and 5 OTUs were found to have incorporated ^{13}C from ^{13}C-cellulose at days 3 and 7, respectively. At days 14 and 30, however, 42 and 39 OTUs were found to incorporate ^{13}C from ^{13}C-cellulose into biomass. An average 16% of the ^{13}C-cellulose added was respired within the first 7 days, 38% by day 14, and 60% by day 30. A *Cellvibrio* and *Sandaracinaceae* OTU assimilated ^{13}C from ^{13}C-cellulose at day 3. Day 7 ^{13}C-cellulose responders included the same *Cellvibrio* responder as day 3, a *Verrucomicrobia* OTU and three *Chloroflexi* OTUs. 50% of Day 14 responders belong to *Proteobacteria* (66% Alpha-, 19% Gamma-, and 14% Beta-) followed by 17% *Planctomycetes*, 14% *Verrucomicrobia*, 10% *Chloroflexi*, 7% *Actinobacteria* and 2% cyanobacteria. *Bacteroidetes* OTUs begin to incoporate ^{13}C from cellulose at day 30 (13% of day 30 responders). Other day 30 responding phyla include *Proteobacteria* (30% of day 30 responders; 42% Alpha-, 42% Delta, 8% Gamma-, and 8% Beta-), *Planctomycetes* (20%), *Verrucomicrobia* (20%), *Chloroflexi* (13%) and cyanobacteria (3%). *Proteobacteria*, *Verrucomicrobia*, and *Chloroflexi* had relatively high numbers of responders with heavy response across multiple time points (Figure 2).

Proteobacteria represent 46% of all ^{13}C-cellulose responding OTUs identified. *Cellvibrio* accounted for 3% of all proteobacterial ^{13}C-cellulose responding OTUs detected. *Cellvibrio* was one of the first identified cellulose degrading bacteria and was originally described by Winogradsky in 1929 who named it for its cellulose degrading abilities (Boone, 2001). All ^{13}C-cellulose responding *Proteobacteria* share high sequence identity with 16S rRNA genes from sequenced cultured isolates (Table 1) except for "OTU.442" (best cultured isolate match 92% sequence identity in the *Chrondomyces* genus, Table 1) and "OTU.663" (best cultured isolate match outside *Proteobacteria* entirely, *Clostridium* genus, 89% sequence identity, Table 1). Some *Proteobacteria* responders share high sequence identity with type strains for genera known to possess cellulose degraders including *Rhizobium*, *Devosia*, *Stenotrophomonas* and *Cellvibrio*. One *Proteobacteria* OTU shares high sequence identity with a *Brevundimonas* cultured isolate. *Brevundimonas* has not previously been identified as a cellulose degrader, but has been shown to degrade cellouronic acid, an oxidized form of cellulose (Tavernier *et al.*, 2008).

Verrucomicrobia, a cosmopolitan soil phylum often found in high abundance (Fierer *et al.*, 2013), are hypthothesized to degrade polysaccharides in many environments (Fierer *et al.*, 2013; Herlemann *et al.*, 2013; Chin *et al.*, n.d.). *Verrucomicrobia* comprise 16% of the total ^{13}C-cellulose responder OTUs detected. 40% of *Verrucomicrobia* ^{13}C-cellulose responders belong to the uncultured "FukuN18" family originally identified in freshwater lakes (Parveen *et al.*, 2013). The *Verrucomicrobia* OTU with the strongest *Verrucomicrobial* response to ^{13}C-cellulose shared high sequence identity (97%) with an isolate from Norway tundra soil (Jiang *et al.*, 2011) although growth on cellulose was not assessed for this isolate. Only one other ^{13}C-cellulose respond-

ing verrucomicrobium shared high DNA sequence identity with a sequenced type strain, "OTU.638" (Table 1) with *Roseimicrobium gellanilyticum* (100% sequence identity). *Roseimicrobium gellanilyticum* grows on soluble cellulose (Otsuka *et al.*, 2012). The remaining ^{13}C-cellulose *Verrucomicrobia* responders did not share high sequence identity with any cultured isolates (maximum sequence identity with any cultured isolate 93%).

Chloroflexi are traditionally known for metabolically dynamic lifestyles ranging from anoxygenic phototrophy to organohalide respiration (Hug *et al.*, 2013). Recent studies have focused on *Chloroflexi* roles in C cycling (Goldfarb *et al.*, 2011; Cole *et al.*, 2013; Hug *et al.*, 2013) and several *Chloroflexi* utilize cellulose (Goldfarb *et al.*, 2011; Cole *et al.*, 2013; Hug *et al.*, 2013). Four closely related OTUs in an undescribed *Chloroflexi* lineage (closest matching cultured isolate for all four OTUs: *Herpetosiphon geysericola*, 89% sequence identity, Table 1) responded to ^{13}C-cellulose (Figure 4). One additional OTU also from a poorly characterized *Chloroflexi* lineage (closest cultured isolate match a proteobacterium at 78% sequence identity) responded to ^{13}C-cellulose (Figure 4).

Other notable ^{13}C-cellulose responders include a *Bacteroidetes* OTU that shares high sequence identity (99%) to *Sporocytophaga myxococcoides* a known cellulose degrader (Vance *et al.*, 1980), and three *Actinobacteria* OTUs that share high sequence identity (100%) with sequenced cultured isolates. One of the three *Actinobacteria* ^{13}C-cellulose responders is in the *Streptomyces*, a genus known to possess cellulose degraders, while the other two share high sequence identity to cultured isolates *Allokutzneria albata* (Tomita *et al.*, 1993; Labeda and Kroppenstedt, 2008) and *Lentzea waywayandensis* (LABEDA and LYONS, 1989; Labeda *et al.*, 2001); neither isolate decomposes cellulose in culture. Nine *Plantomycetes* OTUs responded to ^{13}C-cellulose but none are within described genera (closest cultured isolate match 91% sequence identity, Table 1) (Figure 4). Interestingly, one ^{13}C-cellulose responder is annotated as "cyanobacteria". The cyanobacteria phylum annotation is misleading as the OTU is not closely related to any oxygenic phototrophs (closest cultured isolate match *Vampirovibrio chlorellavorus*, 95% sequence identity, Table 1). A sister clade to the oxygenic phototrophs classically annotated as "cyanobacteria" in SSU rRNA gene reference databases but does not possess any known phototrophs has recently been proposed to constitute its own phylum, "Melainabacteria" Rienzi *et al.* (2013). Although the phylogenetic position of "Melainabacteria" is debated (Soo *et al.*, 2014). The catalog of metabolic capabilities associated with cyanobacteria (or candidate phyla previously annotated as cyanobacteria) are quickly expanding (Rienzi *et al.*, 2013; Soo *et al.*, 2014). Our findings provide evidence for cellulose degradation within a lineage closely related to but apart from oxygenic phototrophs. Notably, polysaccharide degradation is suggested by an analysis of a "Melainabacteria" genome (Rienzi *et al.*, 2013). Although we highlight ^{13}C-cellulose responders that share high sequence identity with described genera, most ^{13}C-cellulose responders uncovered in this experiment are not closely related to cultured isolates (Table 1).

Putative spore-formers in the Firmicutes assimilate ^{13}C from xylose within first day after soil amendment followed by Bacteroidetes and then Actinobacteria OTUs. Within the first 7 days of incubation 63% on average of ^{13}C-xylose was respired and only an additional 6% more was respired from day 7 to 30. At the end of the 30 day incubation 30% of the ^{13}C from added xylose remained in the soils. The ^{13}C remaining in the soil from ^{13}C-xylose addition was likely stabilized by assimilation into microbial biomass and/or microbial conversion into other forms of organic matter. It is also possible that some ^{13}C-xylose remains unavail-

able to microbes due to abiotic interactions in soil (Kalbitz *et al.*, 2000).

At day 1, 84% of ^{13}C-xylose responsive OTUs belong to *Firmicutes*, 11% to *Proteobacteria* and 5% to *Bacteroidetes*. At day 3, *Firmicutes* responders decreased to 5% (from 16 OTUs to 1) while *Bacteroidetes* increased to 63% (from 1 to 12 OTUs) of day 3 responders. The remaining day 3 responders are members of the *Proteobacteria* (26%) and the *Verrucomicrobia* (5%). Day 7 responders were 53% *Actinobacteria*, 40% *Proteobacteria*, and 7% *Firmicutes*. The identities of ^{13}C-xylose responders change with time. The numerically dominant ^{13}C-xylose responder phylum shifts from *Firmicutes* to *Bacteroidetes* and then to *Actinobacteria* across days 1, 3 and 7 (Figure 2, Figure 3).

All of the ^{13}C-xylose responders in the *Firmicutes* phylum are closely related (at least 99% sequence identity) to cultured isolates from genera that are known to form endospores (Table 2). Each ^{13}C-xylose responder is closely related to isolates annotated as members of *Bacillus*, *Paenibacillus* or *Lysinibacillus*. *Bacteroidetes* ^{13}C-xylose responders are predominantly closely related to *Flavobacterium* species (5 of 8 total responders) (Table 2). Only one *Bacteroidetes* ^{13}C-xylose responder is not closely related to a cultured isolate, "OTU.183" (closest LTP BLAST hit, *Chitinophaca sp.*, 89.5% sequence identity, Table 2). OTU.183 shares high sequence identity with environmental clones derived from rhizosphere samples (accession AM158371, unpublished) and the skin microbiome (accession JF219881, Kong *et al.* (2012)). Other *Bacteroidetes* responders share high sequence identities with canonical soil genera including *Dyadobacer*, *Solibius* and *Terrimonas*. Six of the 8 *Actinobacteria* ^{13}C-xylose responders are in the *Micrococcales* order. One ^{13}C-xylose responding *Actinobacteria* OTU shares 100% sequence identity with *Agromyces ramosus* (Table 2). *A. ramosus* is a known predatory bacterium but is not dependent on a host for growth in culture (Casida, n.d.). It is not possible to determine the specific origin of assimilated ^{13}C in a DNA-SIP experiment. ^{13}C can be passed down through trophic levels although heavy isotope representation in C pools targeted by cross-feeders and predators would be diluted with depth into the trophic cascade. It's possible, however, that the ^{13}C labeled *Agromyces* OTU was assimilating ^{13}C primarily by predation if the *Agromyces* OTU was selective enough with respect to its prey that it primarily attacked ^{13}C-xylose assimilating organisms and that those ^{13}C-xylose assimilating organisms utilized ^{13}C-xylose as a sole carbon source.

Cellulose degrader DNA shifts further along the BD gradient upon ^{13}C incorporation than xylose degrader DNA. Cellulose responders exhibited a greater shift in BD than xylose responders in response to isotope incorporation (Figure 5, p-value 1.86e^{-06}). ^{13}C-cellulose responders shifted on average 0.0163 g/mL (sd 0.0094) whereas xylose responders shifted on average 0.0097 (sd 0.0094). For reference, 100% ^{13}C DNA shifts X.XX g/mL relative to the BD of its ^{12}C counterpart. DNA BD increases as its ratio of ^{13}C to ^{12}C increases. An organism that only assimilates C into DNA from a ^{13}C isotopically labeled source, will have a greater ^{13}C:^{12}C ratio in its DNA than an organism utilizing a mixture of isotopically labeled and unlabeled C sources. Upon labeling, DNA from an organism that incorporates exclusively ^{13}C will increase in buoyant density more than DNA from an organism that does not exclusively utilize isotopically labeled C. Therefore the magnitude DNA buoyant density shifts indicate substrate specificity given our experimental design as only one substrate was labeled in each amendment. We measured density shift as the change in an OTU's density profile center of mass between corresponding contol and labeled gradients. Density shifts, however, should not be evaluated on an individual OTU basis as a small number of density shifts are observed for each OTU and the

variance of the density shift metric at the level of individual OTUs is unknown. It is therefore more informative to compare density shifts among substrate responder groups. Further, density shifts are based on relative abundance profiles and would be theoretically muted in comparison to density shifts based on absolute abundance profiles and should be interpreted with this transformation in mind. It should also be noted that there was overlap in observed density shifts between ^{13}C-cellulose and ^{13}C-xylose responder groups suggesting that although cellulose degraders are generally more substrate specific than xylose utilizers, some cellulose degraders show less substrate specificity for cellulose than some xylose utilizers for xylose (Figure 5), and, each responder group exhibits a range of substrate specificites (Figure 5).

Xylose responders at day 1 have more estimated rRNA operon copy numbers per genome than xylose responders at days 3 and 7, and, Xylose responders have more rRNA operon copy numbers than cellulose responders.. ^{13}C-xylose responder rRNA operon genome copy number is inversely related to time of first response (p-value 2.02e^{-15}, Figure 6). OTUs that first respond at later time points have fewer estimated rRNA operons per genome than OTUs that first respond earlier (Figure 6). rRNA operon copy number estimation is a recent advance in microbiome science (Kembel *et al.*, 2012) while the relationship of rRNA operon copy number per genome with ecological strategy is well established (Klappenbach *et al.*, 2000). Microorganisms with a high number of rRNA operons per genome tend to be fast growers specialized to take advantage of boom-bust environments whereas microorganisms with low rRNA operon copy numbers per genome favor slower growth under lower and more consistent nutrient input (Klappenbach *et al.*, 2000). At the beginning of our incubation, OTUs with estimated high rRNA operon copy numbers per genome or "fast-growers" assimilate xylose into biomass and with time slower growers (lower rRNA operon number per genome) begin to respond to the xylose addition. Further, ^{13}C-xylose responders have more estimated rRNA operon copy numbers per genome than ^{13}C-cellulose responders (p-value 1.878e^{-09}) suggesting xylose respiring microbes are generally faster growers than cellulose degraders.

Xylose responders are more abundant in the soil community than cellulose responders. ^{13}C-xylose responders are generally more abundant members based on relative abundance in bulk DNA SSU rRNA gene content than ^{13}C-cellulose responders (Figure 5, p-value 0.00028). However, both abundant and rare OTUs responded to ^{13}C-xylose and ^{13}C-cellulose (Figure 5). For instance, a *Delftia* ^{13}C-cellulose responder is fairly abundant in the bulk samples ("OTU.5", Table 1). OTU.5 was on average the 13th most abundant OTU in bulk samples. A ^{13}C-xylose responder ("OTU.1040", Table 2) has a mean relative abundance in bulk samples of 3.57e^{-05}. Two ^{13}C-cellulose responders wer not found in any bulk samples ("OTU.862" and "OTU.1312", Table 1). Of the 10 most abundant responders 8 are ^{13}C-xylose responders and 6 of these 8 are consistently among the 10 most abundant OTUs in bulk samples.

Variation in bulk soil DNA microbial community structure is significantly less than variation in gradient fractions. Using a distance metric that incorporates relative abundance information (weighted Unifrac metric, (Lozupone and Knight, 2005)) bulk sample beta diversity was less than gradient fraction beta diversity (p-value 0.003). Time was significantly correlated to bulk sample phylogenetic profile variation (p-value 0.23, R^2 0.63, Figure 7) but the contrast between only ^{12}C additions with additions that included isotopically labeled substrates was not (p-value 0.35). When responder abundances were summed within phyla for

[13]C-cellulose and ^{13}C-xylose, summed resonder abundaces generally increased for ^{13}C-cellulose and *Firmicutes*, *Bacteroidetes*, *Actinobacteria* and *Proteobacteria*, the numerically dominant ^{13}C-xylose responder phyla, decreased over time although *Proteobacteria* spiked at day 14 (Figure 8). Bulk abundance trends are roughly consistent with ^{13}C assimilation activity.

Methods

Additional information on sample collection and analytical methods is provided in SI Materials and Methods.

Twelve soil cores (5 cm diameter x 10 cm depth) were collected from six random sampling locations within an organically managed agricultural field in Penn Yan, New York. Soils were pretreated by sieving (2 mm), homogenizing sieved soil, and pre-incubating 10 g of dry soil weight in flasks for 2 weeks. Soils were amended with a 5.3 mg g soil^{-1} carbon mixture; representative of natural concentrations Schneckenberger *et al.*, 2008. Mixture contained 38% cellulose, 23% lignin, 20% xylose, 3% arabinose, 1% galactose, 1% glucose, and 0.5% mannose by mass, with the remaining 13.5% mass composed of an amino acid (in-house made replica of Teknova C0705) and basal salt mixture (Murashige and Skoog, Sigma Aldrich M5524). Three parallel treatments were performed; (1) unlabeled control,(2)[13]C-cellulose, (3)[13]C-xylose (98 atom% [13]C, Sigma Aldrich). Each treatment had 2 replicates per time point (n = 4) except day 30 which had 4 replicates; total microcosms per treatment n = 12, except ^{13}C-cellulose which was not sampled at day 1, n = 10. Other details relating to substrate addition can be found in SI. Microcosms were sampled destructively (stored at -80°C until nucleic acid processing) at days 1 (control and xylose only), 3, 7, 14, and 30.

Nucleic acids were extracted using a modified Griffiths procotol Griffiths *et al.*, 2000. To prepare nucleic acid extracts for isopycnic centrifugation as previously described Buckley *et al.*, 2007, DNA was size selected (>4kb) using 1% low melt agarose gel and β-agarase I enzyme extraction per manufacturers protocol (New England Biolab, M0392S). For each time point in the series isopycnic gradients were setup using a modified protocol Neufeld *et al.*, 2007 for a total of five ^{12}C-control, five ^{13}C-xylose, and four ^{13}C-cellulose microcosms. A density gradient (average density 1.69 g mL^{-1}) solution of 1.762 g cesium chloride (CsCl) ml^{-1} in gradient buffer solution (pH 8.0 15 mM Tris-HCl, 15 mM EDTA, 15 mM KCl) was used to separate ^{13}C-enriched and ^{12}C-nonenriched DNA. Each gradient was loaded with approximately 5 μg of DNA and ultracentrifuged for 66 h at 55,000 rpm and room temperature (RT). Fractions of ~100 μL were collected from below by displacing the DNA-CsCl-gradient buffer solution in the centrifugation tube with water using a syringe pump at a flow rate of 3.3 μL s^{-1} Manefield *et al.*, 2002 into Acroprep^{TM} 96 filter plate (Pall Life Sciences 5035). The refractive index of each fraction was measured using a Reichart AR200 digital refractometer modified as previously described Buckley *et al.*, 2007 to measure a volume of 5 μL. Then buoyant density was calculated from the refractive index as previously described Buckley *et al.*, 2007 (see also SI). The collected DNA fractions were purified by repetitive washing of Acroprep filter wells with TE. Finally, 50 μL TE was added to each fraction then resuspended DNA was pipetted off the filter into a new microfuge tube.

For every gradient, 20 fractions were chosen for sequencing between the density range 1.67-1.75 g mL^{-1}. Barcoded 454 primers were designed using 454-specific adapter B, 10 bp barcodes Hamady *et al.*, 2008, a 2 bp linker (5'-CA-3'), and 806R primer for reverse primer (BA806R); and 454-specific adapter A, a 2 bp linker (5'-TC-3'), and 515F primer for forward primer (BA515F). Each fraction was PCR amplified using 0.25 μL 5 U μl^{-1} AmpliTaq Gold (Life Technologies, Grand Island, NY; N8080243),

2.5 μL 10X Buffer II (100 mM Tris-HCl, pH 8.3, 500 mM KCl), 2.5 μL 25 mM MgCl$_2$, 4 μL 5 mM dNTP, 1.25 μL 10 mg mL^{-1} BSA, 0.5 μL 10 μM BA515F, 1 μL 5 μM BA806R, 3 μL H$_2$O, 10 μL 1:30 DNA template) in triplicate. Samples were normalized either using Pico green quantification and manual calculation or by SequalPrep^{TM} normalization plates (Invitrogen, Carlsbad, CA; A10510), then pooled in equimolar concentrations. Pooled DNA was gel extracted from a 1% agarose gel using Wizard SV gel and PCR clean-up system (Promega, Madison, WI; A9281) per manufacturer's protocol. Amplicons were sequenced on Roche 454 FLX system using titanium chemistry at Selah Genomics (formerly EnGenCore, Columbia, SC)

References

Academic Press.

Allison, SD, Martiny, JBH. (2008). Resistance resilience, and redundancy in microbial communities. *Proc Natl Acad Sci USA* **105:** 11512–11519.

Amundson, R. (2001). T HE C ARBON B UDGET IN S OILS. *Ann Rev Earth Planet Sci* **29:** 535–562.

Angel, R, Conrad, R. (2013). Elucidating the microbial resuscitation cascade in biological soil crusts following a simulated rain event. *Environ Microbiol*. n/a–n/a.

BATJES, N. (1996). Total carbon and nitrogen in the soils of the world. *European Journal of Soil Science* **47:** 151–163.

Boone, D. (2001). Bergey's manual of systematic bacteriology. Springer: New York.

Buckley, DH, Huangyutitham, V, Hsu, SF, Nelson, TA. (2007). Stable Isotope Probing with 15N Achieved by Disentangling the Effects of Genome G+C Content and Isotope Enrichment on DNA Density. *Appl Environ Microbiol* **73:** 3189–3195.

Casida, L. Interaction of Agromyces ramosus with Other Bacteria in Soil. *Appl Environ Microbiol* **46:** 881–8.

Chapin, F. (2002). Principles of terrestrial ecosystem ecology. Springer: New York.

Chen, Y, Murrell, JC. (2010). When metagenomics meets stable-isotope probing: progress and perspectives. *Trends in Microbiology* **18:** 157–163.

Chin, K, Hahn, D, Hengstmann, U, Liesack, W, Janssen, P. Characterization and identification of numerically abundant culturable bacteria from the anoxic bulk soil of rice paddy microcosms. **65:** 5042–9.

Cole, JK, Gieler, BA, Heisler, DL, Palisoc, MM, Williams, AJ, Dohnalkova, AC, *et al.* (2013). Kallotenue papyrolyticum gen. nov. sp. nov., a cellulolytic and filamentous thermophile that represents a novel lineage (Kallotenuales ord. nov., Kallotenuaceae fam. nov.) within the class Chloroflexia. *INTERNATIONAL JOURNAL OF SYSTEMATIC AND EVOLUTIONARY MICROBIOLOGY* **63:** 4675–4682.

DAVIDSON, EA, JANSSENS, IA, LUO, Y. (2006). On the variability of respiration in terrestrial ecosystems: moving beyond Q10. *Global Change Biol* **12:** 154–164.

Fierer, N, Ladau, J, Clemente, JC, Leff, JW, Owens, SM, Pollard, KS, *et al.* (2013). Reconstructing the Microbial Diversity and Function of Pre-Agricultural Tallgrass Prairie Soils in the United States. *Science* **342:** 621–624.

Friedlingstein, P, Cox, P, Betts, R, Bopp, L, Bloh, W von, Brovkin, V, *et al.* (2006). Climate–Carbon Cycle Feedback Analysis: Results from the C 4 MIP Model Intercomparison. *Journal of Climate* **19:** 3337–3353.

Goldfarb, KC, Karaoz, U, Hanson, CA, Santee, CA, Bradford, MA, Treseder, KK, *et al.* (2011). Differential Growth Responses of Soil Bacterial Taxa to Carbon Substrates of Varying Chemical Recalcitrance. *Frontiers in Microbiology* **2:**

Griffiths, RI, Whiteley, AS, O'Donnell, AG, Bailey, MJ. (2000). Rapid Method for Coextraction of DNA and RNA from Natu-

ral Environments for Analysis of Ribosomal DNA- and rRNA-Based Microbial Community Composition. *Appl Environ Microbiol* **66:** 5488–5491.

Groenigen, KJ, Graaff, MA, Six, J, Harris, D, Kuikman, P, Kessel, C. (2006). The Impact of Elevated Atmospheric [CO2] on Soil C and N Dynamics: A Meta-Analysis. In: Managed ecosystems and co2. Springer Science + Business Media, pp. 373–391.

Hamady, M, Walker, JJ, Harris, JK, Gold, NJ, Knight, R. (2008). Error-correcting barcoded primers for pyrosequencing hundreds of samples in multiplex. *Nat Meth* **5:** 235–237.

Herlemann, DPR, Lundin, D, Labrenz, M, Jurgens, K, Zheng, Z, Aspeborg, H, *et al.* (2013). Metagenomic De Novo Assembly of an Aquatic Representative of the Verrucomicrobial Class Spartobacteria. *mBio* **4:**

Hu, S, Bruggen, A van. (1997). Microbial Dynamics Associated with Multiphasic Decomposition of 14 C-Labeled Cellulose in Soil. *Microb Ecol* **33:** 134–143.

Hug, LA, Castelle, CJ, Wrighton, KC, Thomas, BC, Sharon, I, Frischkorn, KR, *et al.* (2013). Community genomic analyses constrain the distribution of metabolic traits across the Chloroflexi phylum and indicate roles in sediment carbon cycling. *Microbiome* **1:** 22.

Jiang, F, Li, W, Xiao, M, Dai, J, Kan, W, Chen, L, *et al.* (2011). Luteolibacter luojiensis sp. nov. isolated from Arctic tundra soil, and emended description of the genus Luteolibacter. *INTERNATIONAL JOURNAL OF SYSTEMATIC AND EVOLUTIONARY MICROBIOLOGY* **62:** 2259–2263.

Kalbitz, K, Solinger, S, Park, JH, Michalzik, B, Matzner, E. (2000). CONTROLS ON THE DYNAMICS OF DISSOLVED ORGANIC MATTER IN SOILS: A REVIEW. *Soil Science* **165:** 277–304.

Kembel, SW, Wu, M, Eisen, JA, Green, JL. (2012). Incorporating 16S Gene Copy Number Information Improves Estimates of Microbial Diversity and Abundance. *PLoS Computational Biology* **8:** ed. by C von Mering. e1002743.

Klappenbach, JA, Dunbar, JM, Schmidt, TM. (2000). rRNA Operon Copy Number Reflects Ecological Strategies of Bacteria. *Appl Environ Microbiol* **66:** 1328–1333.

Kong, HH, Oh, J, Deming, C, Conlan, S, Grice, EA, Beatson, MA, *et al.* (2012). Temporal shifts in the skin microbiome associated with disease flares and treatment in children with atopic dermatitis. *Genome Res* **22:** 850–859.

Labeda, DP, Hatano, K, Kroppenstedt, RM, Tamura, T. (2001). Revival of the genus Lentzea and proposal for Lechevalieria gen. nov. *INTERNATIONAL JOURNAL OF SYSTEMATIC AND EVOLUTIONARY MICROBIOLOGY* **51:** 1045–1050.

Labeda, DP, Kroppenstedt, RM. (2008). Proposal for the new genus Allokutzneria gen. nov. within the suborder Pseudonocardineae and transfer of Kibdelosporangium albatum Tomita et al. 1993 as Allokutzneria albata comb. nov. *INTERNATIONAL JOURNAL OF SYSTEMATIC AND EVOLUTIONARY MICROBIOLOGY* **58:** 1472–1475.

LABEDA, DP, LYONS, AJ. (1989). Saccharothrix texasensis sp. nov. and Saccharothrix waywayandensis sp. nov. *International Journal of Systematic Bacteriology* **39:** 355–358.

Lozupone, C, Knight, R. (2005). UniFrac: a New Phylogenetic Method for Comparing Microbial Communities. *Appl Environ Microbiol* **71:** 8228–8235.

Lozupone, CA, Knight, R. (2008). Species divergence and the measurement of microbial diversity. *FEMS Microbiology Reviews* **32:** 557–578.

Lu, Y. (2005). In Situ Stable Isotope Probing of Methanogenic Archaea in the Rice Rhizosphere. *Science* **309:** 1088–1090.

Manefield, M, Whiteley, AS, Griffiths, RI, Bailey, MJ. (2002). RNA Stable Isotope Probing a Novel Means of Linking Microbial Community Function to Phylogeny. *Appl Environ Microbiol* **68:** 5367–5373.

Nannipieri, P, Ascher, J, Ceccherini, MT, Landi, L, Pietramellara, G, Renella, G. (2003a). Microbial diversity and soil functions. *European Journal of Soil Science* **54:** 655–670.

Nannipieri, P, Ascher, J, Ceccherini, MT, Landi, L, Pietramellara, G, Renella, G. (2003b). Microbial diversity and soil functions. *European Journal of Soil Science* **54:** 655–670.

Neff, JC, Asner, GP. (2001). Dissolved Organic Carbon in Terrestrial Ecosystems: Synthesis and a Model. *Ecosystems* **4:** 29–48.

Neufeld, JD, Vohra, J, Dumont, MG, Lueders, T, Manefield, M, Friedrich, MW, *et al.* (2007). DNA stable-isotope probing. *Nat Protoc* **2:** 860–866.

O'Donnell, AG, Seasman, M, Macrae, A, Waite, I, Davies, JT. (2002). Plants and fertilisers as drivers of change in microbial community structure and function in soils. In: Interactions in the root environment: an integrated approach. Springer Netherlands, pp. 135–145.

Otsuka, S, Ueda, H, Suenaga, T, Uchino, Y, Hamada, M, Yokota, A, *et al.* (2012). Roseimicrobium gellanilyticum gen. nov. sp. nov., a new member of the class Verrucomicrobiae. *INTERNATIONAL JOURNAL OF SYSTEMATIC AND EVOLUTIONARY MICROBIOLOGY* **63:** 1982–1986.

Parveen, B, Mary, I, Vellet, A, Ravet, V, Debroas, D. (2013). Temporal dynamics and phylogenetic diversity of free-living and particle-associated Verrucomicrobia communities in relation to environmental variables in a mesotrophic lake. {*FEMS*} *Microbiol Ecol* **83:** 189–201.

Rienzi, SCD, Sharon, I, Wrighton, KC, Koren, O, Hug, LA, Thomas, BC, *et al.* (2013). The human gut and groundwater harbor non-photosynthetic bacteria belonging to a new candidate phylum sibling to Cyanobacteria. *eLIFE* **2:**

Rui, J, Peng, J, Lu, Y. (2009). Succession of Bacterial Populations during Plant Residue Decomposition in Rice Field Soil. *Appl Environ Microbiol* **75:** 4879–4886.

Schimel, J. (1995). Ecosystem Consequences of Microbial Diversity and Community Structure. In: Arctic and alpine biodiversity: patterns causes and ecosystem consequences. Springer Science + Business Media, pp. 239–254.

Schimel, JP, Schaeffer, SM. (2012). Microbial control over carbon cycling in soil. *Frontiers in Microbiology* **3:**

Schneckenberger, K, Demin, D, Stahr, K, Kuzyakov, Y. (2008). Microbial utilization and mineralization of [14C]glucose added in six orders of concentration to soil. *Soil Biol Biochem* **40:** 1981–1988.

Sollins, P, Homann, P, Caldwell, BA. (1996). Stabilization and destabilization of soil organic matter: mechanisms and controls. *Geoderma* **74:** 65–105.

Soo, RM, Skennerton, CT, Sekiguchi, Y, Imelfort, M, Paech, SJ, Dennis, PG, *et al.* (2014). An Expanded Genomic Representation of the Phylum Cyanobacteria. *Genome Biology and Evolution* **6:** 1031–1045.

Strickland, MS, Lauber, C, Fierer, N, Bradford, MA. (2009). Testing the functional significance of microbial community composition. *Ecology* **90:** 441–451.

Tavernier, ML, Delattre, C, Petit, E, Michaud, P. (2008). β-(1,4)-Polyglucuronic Acids - An Overview. {*TOBIOTJ*} **2:** 73–86.

Tomita, K, Hoshino, Y, Miyaki, T. (1993). Kibdelosporangium albatum sp. nov. Producer of the Antiviral Antibiotics Cycloviracins. *International Journal of Systematic Bacteriology* **43:** 297–301.

Vance, I, Topham, CM, Blayden, SL, Tampion, J. (1980). Extracellular Cellulase Production by Sporocytophaga myxococcoides NCIB 8639. *Microbiology* **117:** 235–241.

Verastegui, Y, Cheng, J, Engel, K, Kolczynski, D, Mortimer, S, Lavigne, J, *et al.* (2014). Multisubstrate Isotope Labeling and Metagenomic Analysis of Active Soil Bacterial Communities. *mBio* **5:**

Wohl, DL, Arora, S, Gladstone, JR. (2004). FUNCTIONAL RE-DUNDANCY SUPPORTS BIODIVERSITY AND ECOSYS-TEM FUNCTION IN A CLOSED AND CONSTANT ENVIRON-MENT. *Ecology* **85:** 1534–1540.

Yanagita, T. (1990). Natural microbial communities: ecological and physiological features. Japan Scientific Societies Press. Springer-Verlag.

Figures

Table 1: ^{13}C-cellulose responders BLAST against Living Tree Project

OTU ID	log_2label:control	Genera of top hits	BLAST %ID	Phylum
OTU.862	5.87	Allokutzneria albata	100.0	Actinobacteria
OTU.257	2.94	Lentzea waywayandensis, Lentzea flaviverrucosa	100.0	Actinobacteria
OTU.132	2.81	Streptomyces spp.	100.0	Actinobacteria
OTU.465	3.79	Ohtaekwangia kribbensis	92.73	Bacteroidetes
OTU.1094	3.69	Sporocytophaga myxococcoides	99.55	Bacteroidetes
OTU.669	3.34	Ohtaekwangia koreensis	92.69	Bacteroidetes
OTU.573	3.03	Adhaeribacter aerophilus	92.76	Bacteroidetes
OTU.670	2.87	Adhaeribacter aerophilus	91.78	Bacteroidetes
OTU.64	4.31	Herpetosiphon geysericola	89.5	Chloroflexi
OTU.4322	4.19	Herpetosiphon geysericola	89.14	Chloroflexi
OTU.98	3.68	Herpetosiphon geysericola	88.18	Chloroflexi
OTU.971	3.68	Thiofaba tepidiphila	78.57	Chloroflexi
OTU.5190	3.6	Herpetosiphon geysericola	88.13	Chloroflexi
OTU.120	4.76	Vampirovibrio chlorellavorus	94.52	Cyanobacteria
OTU.1065	5.31	Blastopirellula marina	84.55	Planctomycetes
OTU.484	4.92	Pirellula staleyi DSM 6068	89.09	Planctomycetes
OTU.1204	4.32	Planctomyces limnophilus	91.78	Planctomycetes
OTU.150	4.06	Planctomyces limnophilus	86.76	Planctomycetes
OTU.663	3.63	Pirellula staleyi DSM 6068	90.87	Planctomycetes
OTU.473	3.58	Pirellula staleyi DSM 6068	90.91	Planctomycetes
OTU.285	3.55	Blastopirellula marina	90.87	Planctomycetes
OTU.351	3.54	Pirellula staleyi DSM 6068	91.86	Planctomycetes
OTU.600	3.48	Planctomyces brasiliensis DSM 5305	80.37	Planctomycetes
OTU.11	5.25	Stenotrophomonas pavanii, Stenotrophomonas maltophilia, Pseudomonas geniculata	99.54	Proteobacteria
OTU.900	4.87	Brevundimonas vesicularis, Brevundimonas nasdae	100.0	Proteobacteria
OTU.6062	4.83	Dokdonella sp. DC-3, Luteibacter rhizovicinus	97.26	Proteobacteria
OTU.518	4.8	Hydrogenophaga intermedia	100.0	Proteobacteria
OTU.1754	4.48	Asticcacaulis biprosthecium, Asticcacaulis benevestitus	96.8	Proteobacteria
OTU.982	4.47	Devosia neptuniae	100.0	Proteobacteria
OTU.1087	4.32	Devosia soli, Devosia crocina, Devosia riboflavina	99.09	Proteobacteria
OTU.1312	4.07	Paucimonas lemoignei	99.54	Proteobacteria
OTU.5539	4.01	Devosia subaequoris	98.17	Proteobacteria
OTU.3775	3.88	Devosia glacialis, Devosia chinhatensis, Devosia geojensis, Devosia yakushimensis	98.63	Proteobacteria
OTU.633	3.84	Clostridium cellobioparum	89.5	Proteobacteria
OTU.3594	3.83	Chondromyces robustus	90.41	Proteobacteria
OTU.429	3.7	Devosia limi, Devosia psychrophila	97.72	Proteobacteria
OTU.5	3.69	Delftia tsuruhatensis, Delftia lacustris	100.0	Proteobacteria

Table 1 – continued from previous page

OTU ID	log_2**label:control**	Genera of top hits	BLAST %ID	Phylum
OTU.6	3.62	Cellvibrio fulvus	100.0	Proteobacteria
OTU.119	3.31	Brevundimonas alba	100.0	Proteobacteria
OTU.154	3.24	Pseudoxanthomonas mexicana, Pseudoxanthomonas japonensis	100.0	Proteobacteria
OTU.766	3.21	Devosia insulae	99.54	Proteobacteria
OTU.165	3.1	Rhizobium spp.	100.0	Proteobacteria
OTU.442	3.05	Chondromyces robustus	92.24	Proteobacteria
OTU.32	3.0	Sandaracinus amylolyticus	94.98	Proteobacteria
OTU.327	2.99	Asticcacaulis biprosthecium, Asticcacaulis benevestitus	98.63	Proteobacteria
OTU.90	2.94	Sphingopyxis panaciterrae, Sphingopyxis chilensis, Sphingopyxis sp. BZ30, Sphingomonas sp.	100.0	Proteobacteria
OTU.114	2.78	Herbaspirillum sp. SUEMI03, Herbaspirillum sp. SUEMI10, Oxalicibacterium solurbis, Herminiimonas fonticola, Oxalicibacterium horti	100.0	Proteobacteria
OTU.100	2.66	Pseudoxanthomonas sacheonensis, Pseudoxanthomonas dokdonensis	100.0	Proteobacteria
OTU.28	2.59	Rhizobium giardinii, Rhizobium tubonense, Rhizobium tibeticum, Rhizobium mesoamericanum CCGE 501, Rhizobium herbae, Rhizobium endophyticum	99.54	Proteobacteria
OTU.228	2.54	Sorangium cellulosum	98.17	Proteobacteria
OTU.19	2.44	Rhizobium spp., Arthrobacter spp.	99.54	Proteobacteria
OTU.899	2.28	Enhygromyxa salina	97.72	Proteobacteria
OTU.83	5.61	Luteolibacter sp. CCTCC AB 2010415	97.72	Verrucomicrobia
OTU.1023	4.61	Stenotrophomonas koreensis	80.54	Verrucomicrobia
OTU.266	4.54	Prosthecobacter dejongeii	83.64	Verrucomicrobia
OTU.541	4.49	Verrucomicrobium spinosum	84.23	Verrucomicrobia
OTU.627	4.43	Verrucomicrobiaceae bacterium DC2a-G7	100.0	Verrucomicrobia
OTU.185	4.37	Verrucomicrobium spinosum	85.14	Verrucomicrobia
OTU.638	4.0	Luteolibacter sp. CCTCC AB 2010415, Luteolibacter algae	93.61	Verrucomicrobia
OTU.2192	3.49	Prosthecobacter fluviatilis	83.56	Verrucomicrobia
OTU.1533	3.43	Marvinbryantia formatexigens	82.27	Verrucomicrobia
OTU.241	3.38	Prosthecobacter debontii	87.73	Verrucomicrobia

Table 2: ^{13}C-xylose responders BLAST against Living Tree Project

OTU ID	log_2**label:control**	Genera of top hits	BLAST %ID	Phylum
OTU.5284	3.56	Isoptericola nanjingensis, Isoptericola hypogeus, Isoptericola variabilis	98.63	Actinobacteria
OTU.4446	3.49	Catenuloplanes niger, Catenuloplanes castaneus, Catenuloplanes atrovinosus, Catenuloplanes crispus, Catenuloplanes nepalensis, Catenuloplanes japonicus	97.72	Actinobacteria

Table 2 – continued from previous page

OTU ID	log_2label:control	Genera of top hits	BLAST %ID	Phylum
OTU.252	3.34	Promicromonospora thailandica	100.0	Actinobacteria
OTU.244	3.08	Cellulosimicrobium funkei, Cellulosimicrobium terreum	100.0	Actinobacteria
OTU.4	2.84	Agromyces ramosus	100.0	Actinobacteria
OTU.24	2.81	Cellulomonas aerilata, Cellulomonas humilata, Cellulomonas terrae, Cellulomonas soli, Cellulomonas xylanilytica	100.0	Actinobacteria
OTU.37	2.68	Phycicola gilvus, Microterricola viridarii, Frigoribacterium faeni, Frondihabitans sp. RS-15, Frondihabitans australicus	100.0	Actinobacteria
OTU.62	2.57	Nakamurella flavida	100.0	Actinobacteria
OTU.14	3.92	Flavobacterium oncorhynchi, Flavobacterium glycines, Flavobacterium succinicans	99.09	Bacteroidetes
OTU.277	3.52	Solibius ginsengiterrae	95.43	Bacteroidetes
OTU.6203	3.32	Flavobacterium granuli, Flavobacterium glaciei	100.0	Bacteroidetes
OTU.183	3.31	Chitinophaga sp. YC7001	89.5	Bacteroidetes
OTU.5906	3.16	Terrimonas sp. M-8	96.8	Bacteroidetes
OTU.159	3.16	Flavobacterium hibernum	98.17	Bacteroidetes
OTU.2379	3.1	Flavobacterium pectinovorum, Flavobacterium sp. CS100	97.72	Bacteroidetes
OTU.131	3.07	Flavobacterium fluvii, Flavobacteria bacterium HMD1033, Flavobacterium sp. HMD1001	100.0	Bacteroidetes
OTU.360	2.98	Flavisolibacter ginsengisoli	95.0	Bacteroidetes
OTU.760	2.89	Dyadobacter hamtensis	98.63	Bacteroidetes
OTU.3540	2.52	Flavobacterium terrigena	99.54	Bacteroidetes
OTU.107	2.25	Flavobacterium sp. 15C3, Flavobacterium banpakuense	99.54	Bacteroidetes
OTU.369	5.05	Paenibacillus sp. D75, Paenibacillus glycanilyticus	100.0	Firmicutes
OTU.267	4.97	Paenibacillus pabuli, Paenibacillus tundrae, Paenibacillus taichungensis, Paenibacillus xylanexedens, Paenibacillus xylanilyticus	100.0	Firmicutes
OTU.1040	4.78	Paenibacillus daejeonensis	100.0	Firmicutes
OTU.57	4.39	Paenibacillus castaneae	98.62	Firmicutes
OTU.394	4.06	Paenibacillus pocheonensis	100.0	Firmicutes
OTU.319	3.98	Paenibacillus xinjiangensis	97.25	Firmicutes
OTU.5603	3.96	Paenibacillus uliginis	100.0	Firmicutes
OTU.1069	3.85	Paenibacillus terrigena	100.0	Firmicutes
OTU.843	3.62	Paenibacillus agarexedens	100.0	Firmicutes
OTU.2040	2.91	Paenibacillus pectinilyticus	100.0	Firmicutes
OTU.3	2.61	[Brevibacterium] frigoritolerans, Bacillus sp. LMG 20238, Bacillus coahuilensis m4-4, Bacillus simplex	100.0	Firmicutes
OTU.335	2.53	Paenibacillus thailandensis	98.17	Firmicutes
OTU.3507	2.36	Bacillus spp.	98.63	Firmicutes
OTU.8	2.26	Bacillus niacini	100.0	Firmicutes

Table 2 – continued from previous page

OTU ID	log_2label:control	Genera of top hits	BLAST %ID	Phylum
OTU.4743	2.24	Lysinibacillus fusiformis, Lysinibacillus sphaericus	99.09	Firmicutes
OTU.9	2.04	Bacillus megaterium, Bacillus flexus	100.0	Firmicutes
OTU.68	3.74	Shigella flexneri, Escherichia fergusonii, Escherichia coli, Shigella sonnei	100.0	Proteobacteria
OTU.290	3.59	Pantoea spp., Kluyvera spp., Klebsiella spp., Erwinia spp., Enterobacter spp., Buttiauxella spp.	100.0	Proteobacteria
OTU.346	3.44	Pseudoduganella violaceinigra	99.54	Proteobacteria
OTU.48	2.99	Aeromonas spp.	100.0	Proteobacteria
OTU.22	2.8	Paracoccus sp. NB88	99.09	Proteobacteria
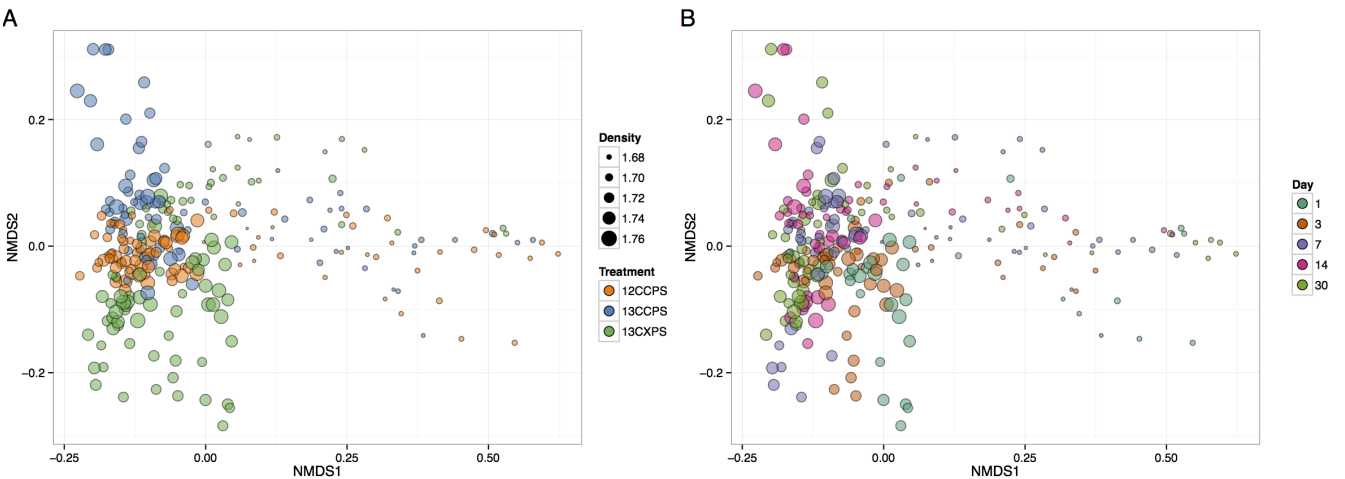
Fig. 1. NMDS analysis from weighted unifrac distances of 454 sequence data from SIP fractions of each treatment over time. Twenty fractions from a CsCl gradient fractionation for each treatment at each time point were sequenced (Fig. S1). Each point on the NMDS represents the bacterial composition based on 16S sequencing for a single fraction where the size of the point is representative of the density of that fraction and the colors represent the treatments (A) or days (B).
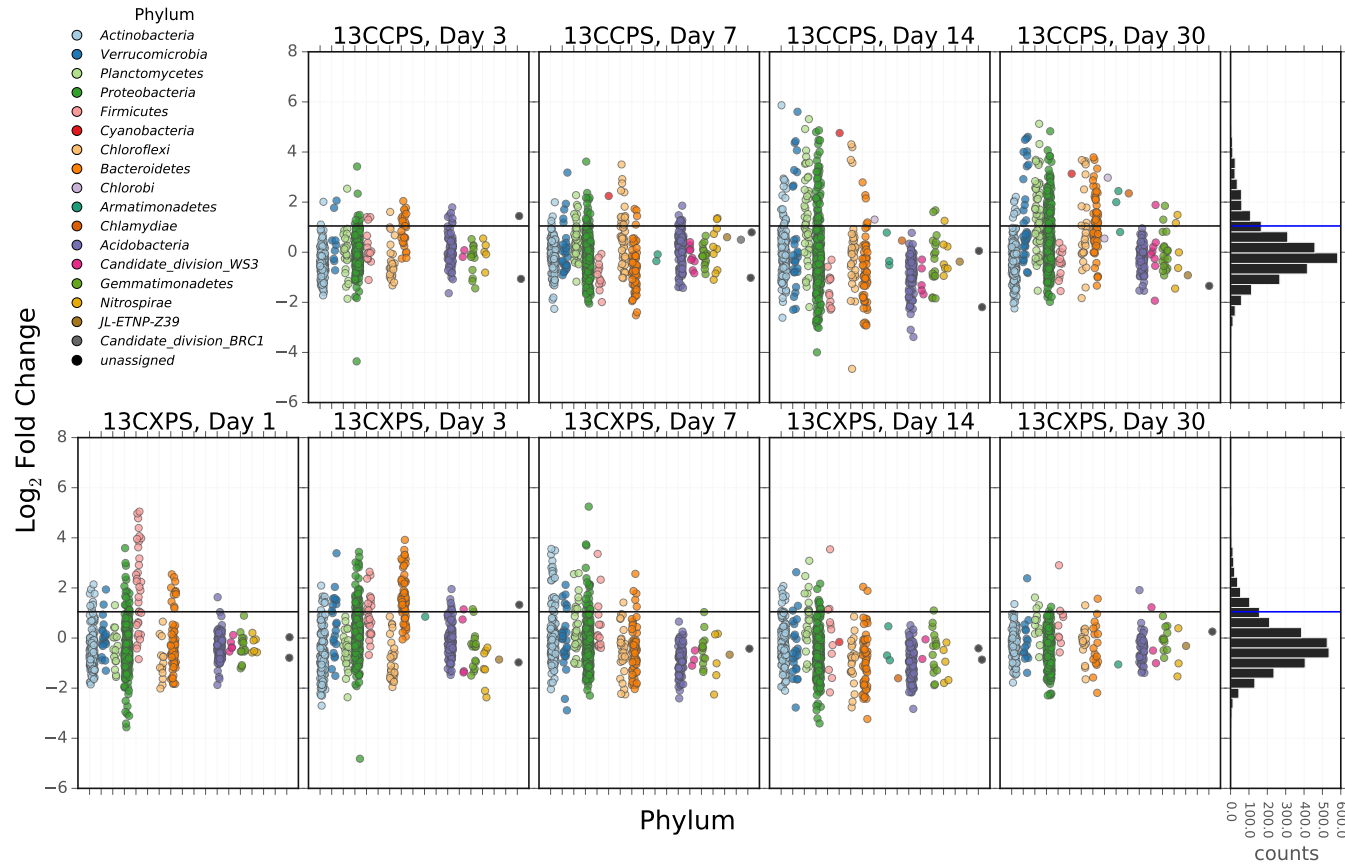
Fig. 2. Log_2 fold change of ^{13}C-responders in cellulose treatment (top) and xylose treatment (bottom). Log_2 fold change is based on the relative abundance in the experimental treatment compared to the control within the density range 1.7125-1.755 g ml^{-1}. Taxa are colored by phylum. 'Counts' is a histogram of number of sequences for each log_2 fold change value.
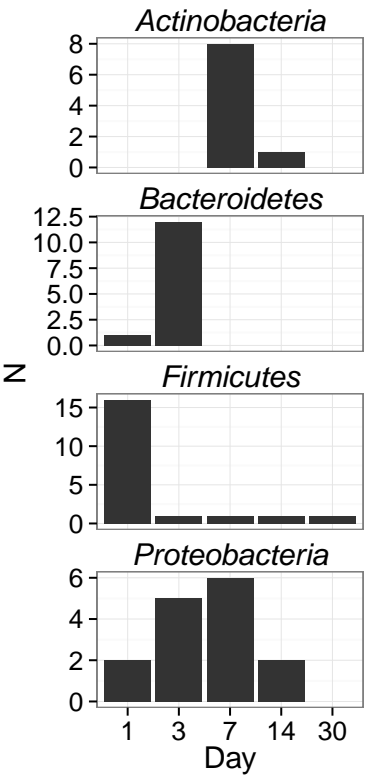
Fig. 3. Counts of ^{13}C-xylose responders in the *Actinobacteria, Bacteroidetes, Firmicutes* and *Proteobacteria* at days 1, 3, 7 and 30.
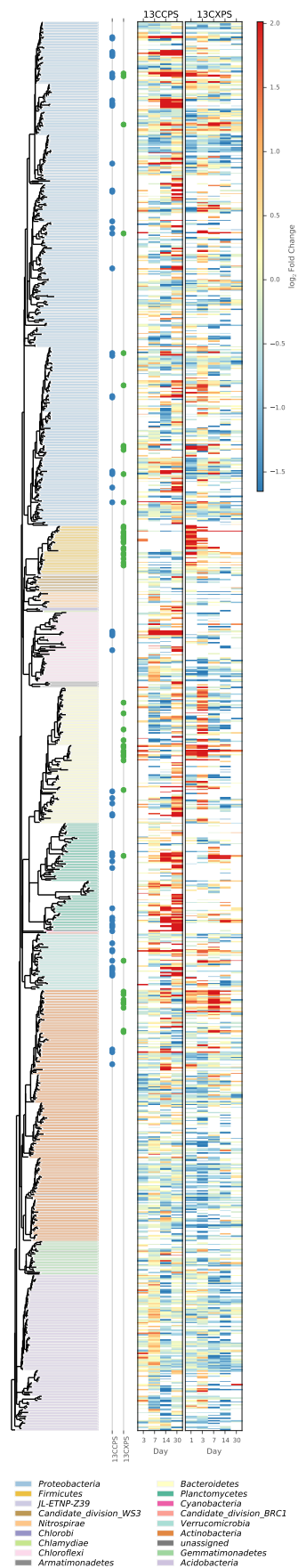
Fig. 4. Phylogenetic tree of sequences passing a user_defined sparcity threshold (0.6) for at least one day of the time series. Branches are colored by phylum. ^{13}C-responders for cellulose (blue) and xylose (green) are indicated by a point beside the respective branch. Heatmap demonstrates log$_2$ fold change of each taxa through the full time series for both treatments (cellulose, left; xylose, right).
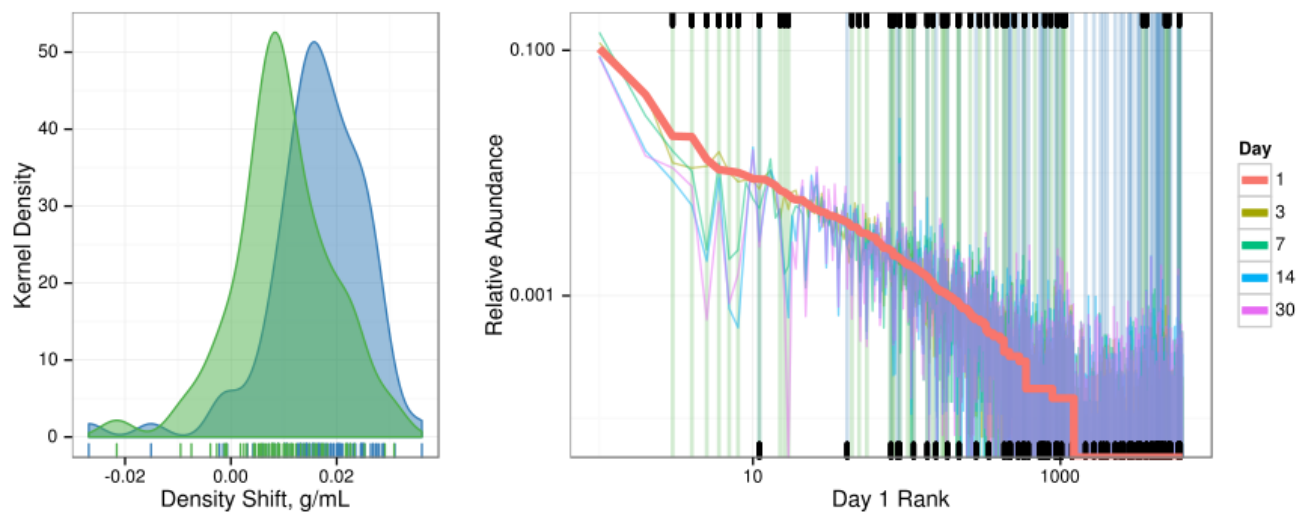
Fig. 5. ^{13}C-responder characteristics based on density shift (A) and rank (B). Kernel density estimation of ^{13}C-responder's density shift in cellulose treatment (blue) and xylose treatment (green) demonstrates degree of labeling for responders for each respective substrate. ^{13}C-responders in rank abundance are labeled by substrate (cellulose, blue; xylose, green). Ticks at top indicate location of ^{13}C-cylose responders in bulk community. Ticks at bottom indicate location of ^{13}C-cellulose responders in bulk community. OTU rank was assessed from day 1 bulk samples.
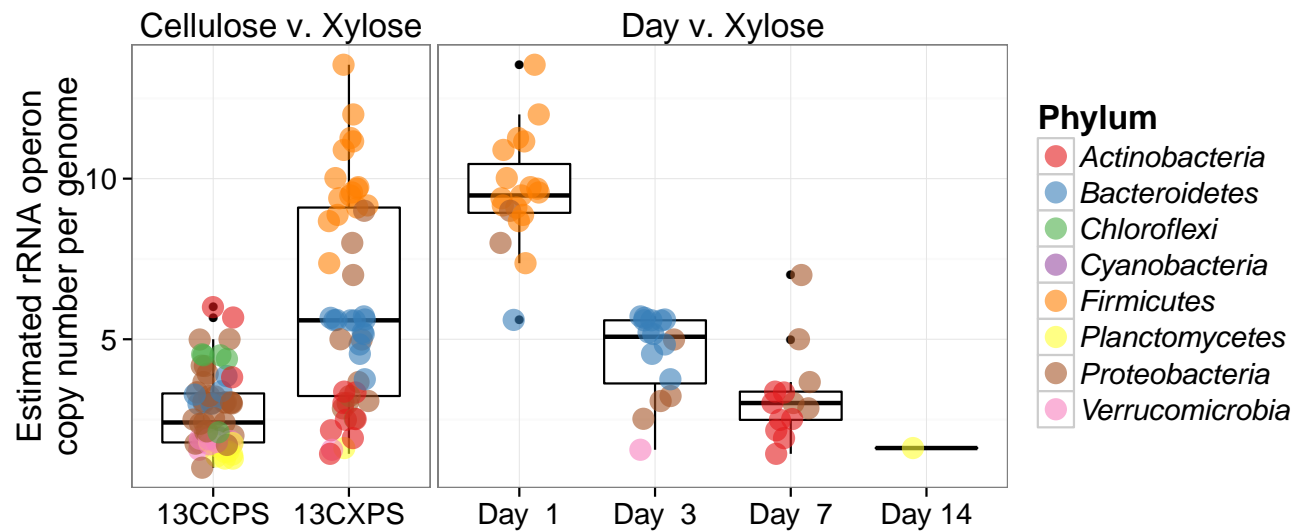
Fig. 6. Estimated rRNA operon copy number per genome for ^{13}C responding OTUS. Panel titles indicate which labeled substrate(s) are depicted.
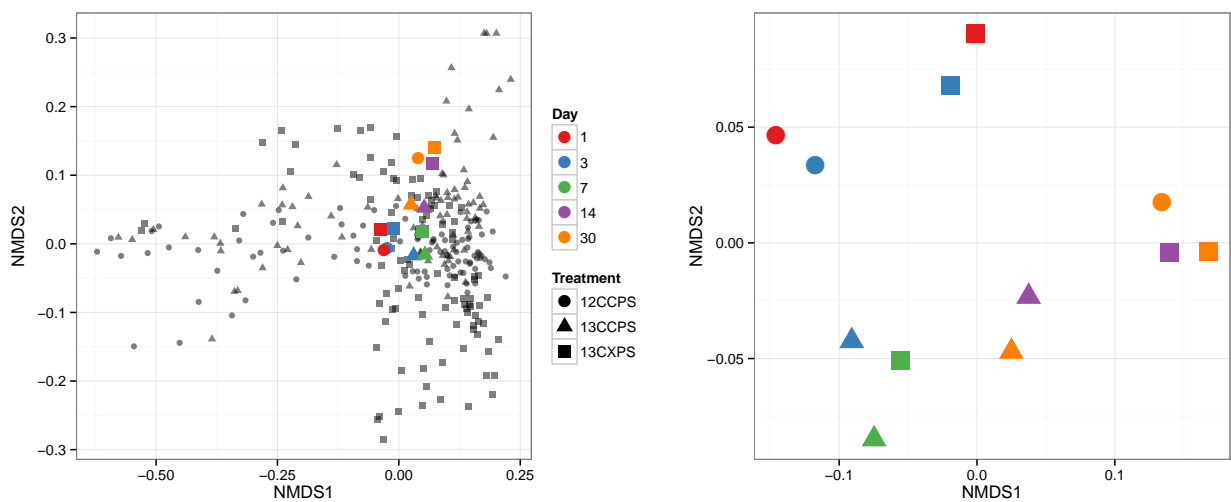
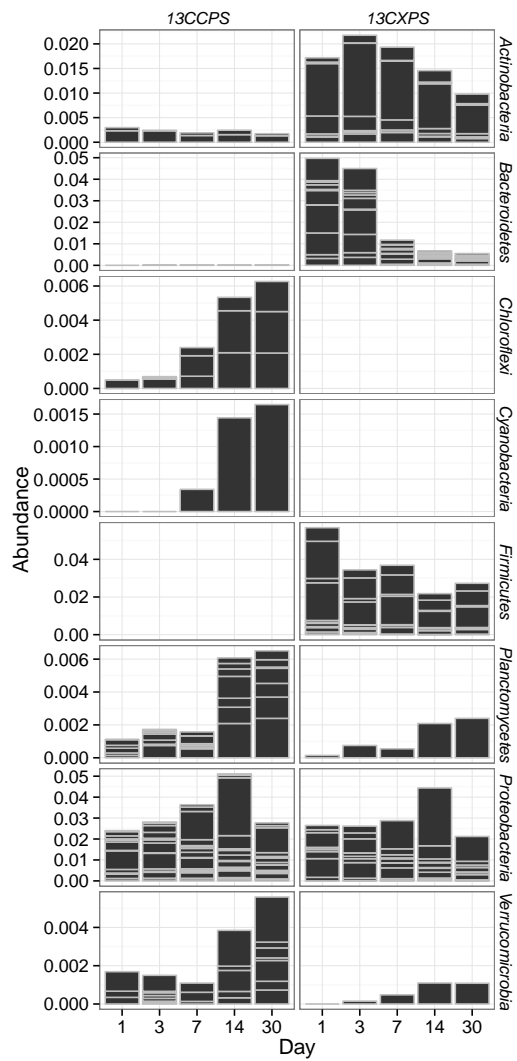**Fig. 7.** Ordination of bulk gradient fraction phylogenetic profiles.

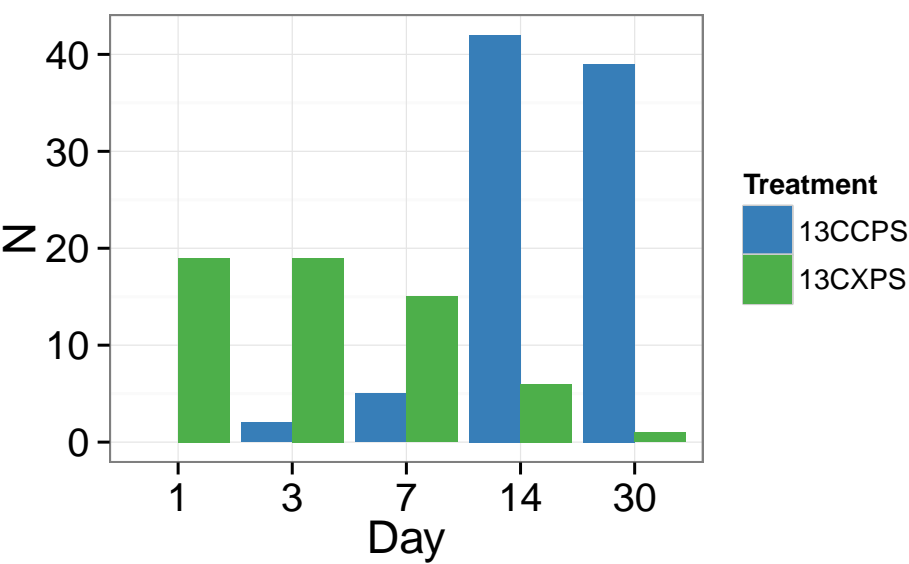**Fig. 8.** Sum of bulk abundances with each phylum for responder OTUs.

Fig. 9. Counts of responders to each isotopically labeled substrate (cellulose and xylose) over time.